Vol 13 No 11, November 2004
1009-1963/2004/13(11)/1936-05

Chinese Physics

© 2004 Chin. Phys. Soc.
and IOP Publishing Ltd

Effects of barium on the nonlinear electrical characteristics and dielectric properties of SnO_2-based varistors*

Wang Chun-Ming(王春明)†, Wang Jin-Feng(王矜奉), Wang Chun-Lei(王春雷), Chen Hong-Cun(陈洪存), Su Wen-Bin(苏文斌), Zang Guo-Zhong(臧国忠), Qi Peng(亓 鹏), Zhao Ming-Lei(赵明磊), and Ming Bao-Quan(明保全)

School of Physics and Microelectronics, National Key Laboratory of Crystal Materials, Shandong University, Jinan 250100, *China*

(Received 31 March 2004; revised manuscript received 14 May 2004)

The effects of barium on electrical and dielectric properties of the SnO_2·Co_2O_3·Ta_2O_5 varistor system sintered at 1250°C for 60min were investigated. It is found that barium significantly improves the nonlinear properties. The breakdown electrical field increases from 378.0 to 2834.5V/mm, relative dielectric constant (at 1kHz) falls from 1206 to 161 and the resistivity (at 1kHz) rises from 60.3 to 1146.5kΩ·cm with an increase of $BaCO_3$ concentration from 0mol% to 1.00mol%. The sample with 1.00mol% barium has the best nonlinear electrical property and the highest nonlinear coefficient (α=29.2). A modified defect barrier model is introduced to illustrate the grain-boundary barrier formation of barium-doped SnO_2-based varistors.

Keywords: varistors, tin oxide, electrical and dielectric properties, barium carbonate
PACC: 7220H, 7280T, 7290

1. Introduction

Varistors are electric devices whose primary functions are to sense and limit transient voltage and to do so repeatedly without being destroyed. A typical multi-component SnO_2-based varistor series is a very complex chemical and physical system. The nonlinear electrical properties of varistors are strongly related to the processing method and chemical constituents. Therefore it is very important to comprehend the effects of the individual additives on both electrical properties and dielectric properties of SnO_2. Small quantities of additives in varistors tremendously influence the grain boundary-related properties. The grain boundary layer modifiers alter the point defect distribution at the grain boundaries and the solute segregation. To obtain better properties, several dopants (such as MnO_2, CoO, Sb_2O_3) have been proposed to modify the varistors.[1−3] It is clear that the sintering behaviour of the SnO_2-based varistors can be strongly modified by the addition of several oxides. In recent years, the effects of barium (since the $BaCO_3$ decomposed into BaO during sintering[4]) on the ZnO-based and TiO_2-based varistors have been investigated. It was found that barium can improve the threshold voltage of the varistors[5−8] and the varistors doped with this oxide are promising materials for ultrahigh voltage protection. The goal of the present work is to investigate the influence of $BaCO_3$ additives on the electrical properties, the dielectric properties, and the defect structure of the SnO_2·Co_2O_3·Ta_2O_5 varistor system. It is found that $BaCO_3$ affects significantly the threshold voltage, the electrical and dielectric properties. Also the high nonlinear coefficient α=29.2 is obtained.

2. Experimental procedure

Nonohmic SnO_2-based varistors were prepared by the conventional ceramic fabrication procedure. Appropriate amounts of raw chemicals, SnO_2 (analytical grades, 99.5% purity), Co_2O_3 (analytical grades, 99% purity), Ta_2O_5 (analytical grades, 99.5% pu-

*Project supported by the Natural Science Foundation of Shandong Province, China (Grant No Z2003F04).
†Corresponding author: E-mail: sdwangcm@mail.edu.cn or sdwangcm@mail.sdu.edu.cn (Chun-Ming Wang)

rity) and $BaCO_3$ (analytical grades, 99.5% purity), were weighed according to the molar ratio of Co_2O_3: Ta_2O_5: $BaCO_3$: SnO_2=0.75: 0.10: x: (99.15-x), where x= 0.00, 0.10, 0.25, 0.50 and 1.00. The samples were ground and pressed into discs of 15mm in diameter and 1.0mm thick. They were sintered at a temperature of 1250°C for 60min and then cooled to room temperature freely. The ceramic phases analysis was conducted by x-ray diffraction (XRD). The sintered density values are obtained by the Archimedes method. For electrical properties measurement, silver electrodes were fixed on both surfaces of the sintered pellets. And for electrical characterization of the current density versus applied electrical field, a semiconductor I–V graph (QT2) and a 2410 high-voltage source meter (Keithley) were used. The impedance measurements were performed with an HP4294A impedance analyser (Agilent).

3. Results and discussion

The XRD analysis was performed and no obvious second phases other than SnO_2 were observed; this phenomenon is similar to that reported by Bacelar *et al*[9] and Wang *et al*.[10] The reason for the absence of apparent second phases is probably that so little amount of barium was added that other phases produced by dopants are not detected in normal XRD patterns, which is distinct to ZnO-based varistors.

The sintered density values are obtained by the Archimedes method and related to the theoretical density of SnO_2 (=6.95g·cm^{-3}), as listed in Table 1. It is found that the density of the samples decreases with the barium concentration, this implies that the barium significantly affects the mass transport and makes the density decrease with concentration. But the fact that the relative density of all samples is obtained prefigures that SnO_2-based varistors are possible candidates for many dense industrial applications.

The nonlinear coefficient α was obtained by[11]

$$\alpha = \frac{\log(I_2/I_1)}{\log(V_2/V_1)}, \qquad (1)$$

where V_1 and V_2 are the voltages at currents I_1 and I_2, respectively. Figure 1 shows the electrical characteristics of $BaCO_3$-doped SnO_2-based varistors. All the samples have excellent nonlinear curves in the figure. The sample with 1.00mol% $BaCO_3$ has the best nonlinear electrical property and the highest nonlinear coefficient (α=29.2), though its density is not preferable to other samples in that it can influence the current drain. The high value obtained in the system indicates that the SnO_2-based varistors are promising candidates for ZnO-based varistors in commercial applications.

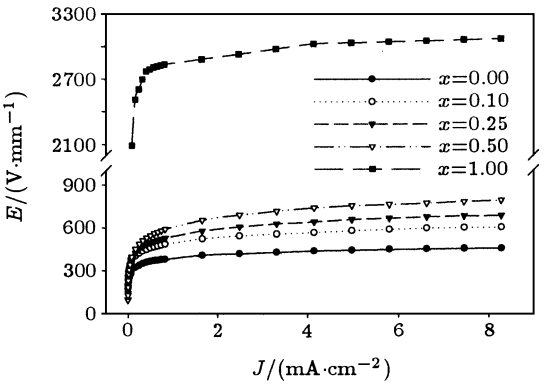


Fig.1. E–J characteristics of samples doped with different concentrations of $BaCO_3$.

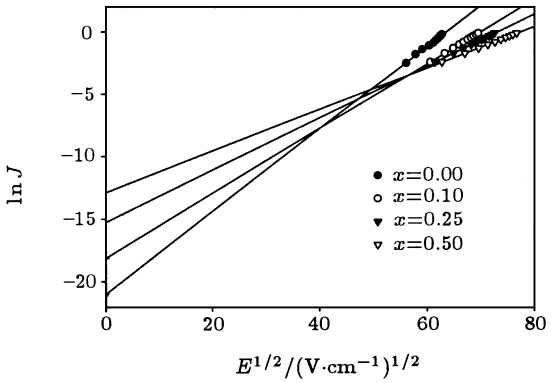


Fig.2. Values of ln$J$ versus $E^{1/2}$ for samples doped with different concentrations of $BaCO_3$.

A grain-boundary defect model for SnO_2-based varistors can be developed, analogous to the band comprising the Schottky barriers. According to this model, the electrical conduction in the ohmic region was associated with the thermionic emission of the Schottky type. For this type of mechanism the current density is related to the electrical field and temperature by the equation[12–14]

$$J = AT^2\exp[(\beta E^{1/2} - \phi_B)/kT], \qquad (2)$$

where A is Richardson's constant, k Boltzmann constant, ϕ_B the interface barrier height, and β a constant related to the grain size and the barrier width:

$$\beta \propto 1/(r \times \omega), \qquad (3)$$

where r is the number of grains per unit length and ω is the voltage barrier width. To obtain the value of ϕ_B, Eq.(2) is converted to the equation

$$\ln J = \ln(AT^2) + (\beta E^{1/2} - \phi_B)/kT. \qquad (4)$$

The plots of $\ln J$ versus $E^{1/2}$ at low current are made to determine values for ϕ_B for all samples, as shown in Fig.2 where J is in unit of $mA \cdot cm^{-2}$. By extrapolating the plots to E=0, the intersection of the extrapolated line with the axis of $\ln J$ can be obtained for all samples. Then, from the value of the intercept, the values of ϕ_B can be derived. The values of ϕ_B are shown in Table 1.

Table 1. Parameters of all the samples sintered at 1250°C for 60min.

mol%	Relative densities/(%)	α	$E/(V \cdot mm^{-1})$	ϕ_B/eV	ε_R (at 1kHz)	$\rho/(k\Omega \cdot cm$ at 1kHz)	tanδ (at 1kHz)
0.00	98.4	12.6	378.0	1.17	1206	60.3	0.049
0.10	97.5	10.7	483.4	1.10	896	63.6	0.032
0.25	96.2	8.9	526.3	1.03	702	86.1	0.033
0.50	94.6	7.8	588.2	0.97	550	116.3	0.036
1.00	86.8	29.2	2834.5	–	161	1146.5	0.105

The relative dielectric constant $\varepsilon/\varepsilon_0$ versus frequency plots for all samples doped with different concentration of $BaCO_3$ are shown in Fig.3. The doping content of $BaCO_3$ has a strong influence on the permittivity and $\varepsilon/\varepsilon_0$ decreases monotonically with increase of the frequency in the range of 40Hz–13MHz. The permittivity of the sample deceases with increasing $BaCO_3$ concentration at the same frequency. The permittivity of all the samples at 1kHz, which is listed in Table 1, is much higher than that of SnO_2 (9.65) or intergranular materials.

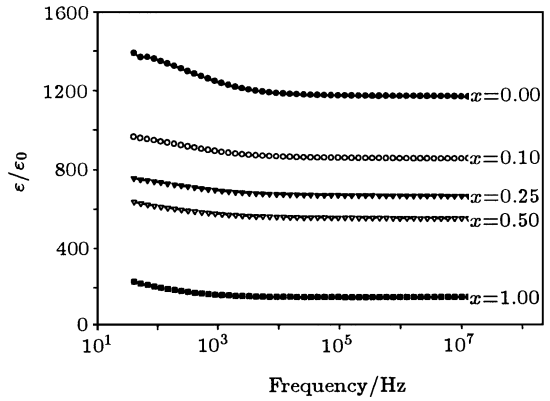


Fig.3. Relative dielectric constant versus frequency for samples doped with different concentrations of $BaCO_3$.

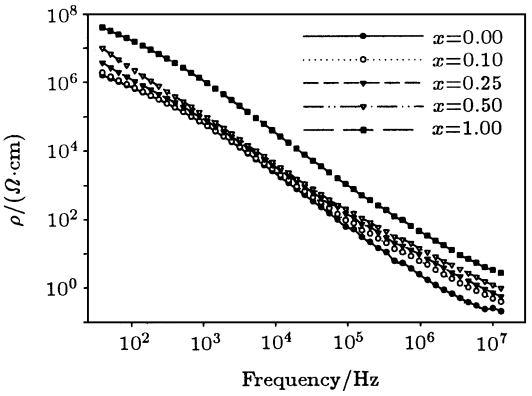


Fig.4. Resistivity versus frequency plots for samples doped with different concentrations of $BaCO_3$.

Figure 4 shows the room temperature resistivity ρ versus frequency plots for the samples. At the frequency of 1kHz the resistivity of the sample increases with increasing $BaCO_3$ concentration, as listed in Table 1. With increase of the frequency in the range of 40Hz–13MHz, it can be seen in each sample that ρ decreases monotonically with increasing frequency.

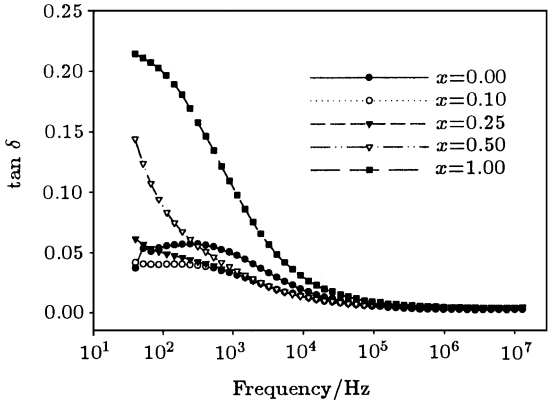


Fig.5. Dielectric loss versus frequency for samples doped with different concentrations of $BaCO_3$.

The dielectric loss tan δ versus frequency plots are illustrated in Fig.5. It can be seen that the dielectric loss tan δ decreases monotonically with increasing frequency from 40Hz to 13MHz but for the sample without doping with barium. Also, it can be seen the dielectric loss of each sample is extraordinarily low, being no more than 0.06 in high frequency region (10k–13MHz), which also indicates at the single-phase of the SnO_2-based varistors. Table 1 lists the values tanδ for all samples at 1kHz.

The $SnO_2 \cdot Co_2O_3 \cdot Ta_2O_5$ varistor system has been studied in the literature.[10,15] It was found that this system exhibits excellent nonlinear properties. The radius of Ba^{2+} (0.134nm) is much larger than that of Sn^{4+} (0.071nm), therefore when $BaCO_3$ is introduced

into SnO_2, Ba^{2+} will substitute Sn^{4+} rather than inhabit the SnO_2 lattice:

$$BaO \xrightarrow{SnO_2} Ba''_{Sn} + V^{\cdot\cdot}_{O} + xO^{\times}_{O} + \frac{1-x}{2}O_2, x = 0 \text{ to } 1, \quad (5)$$

where the Kröger–Vink marks were used. The addition of barium to the $SnO_2{\cdot}Co_2O_3{\cdot}Ta_2O_5$ varistor system increases the resistivity of the grain boundary, as shown in Fig.5 and Table 1, then raises the electrical field E_B. Furthermore, with the quantity of barium increased, the sample becomes highly resistive. Also, the introduction of barium leads to ceramics with higher values of α and hinders the small SnO_2 grains from combining with each other to grow larger, thus inhibiting grain growth. Thus, this oxide should directly influence the grain boundary voltage barrier of this ceramics system. Several studies on the conduction mechanism of ZnO[14,16–18] and SnO_2[19–22] have appeared in the literature. The most remarkable difference in the two varistor systems is in the microstructure aspects. ZnO varistor system is a multiphase one with the ZnO grains as predominant, and several secondary phases such as the spinel phase ($Zn_7Sb_2O_{12}$), pyrochlore ($Zn_2Bi_3Sb_3O_{14}$) and a polymorphic phase of bismuth oxide. Those phases play important role in the formation of the varistor microstructure and, consequently, in its electrical properties. On the other hand, the SnO_2 varistor system is an apparent single phase and its microstructure development occurs by solid state sintering. This means that dopant solid solution or solid-state phase precipitation at grain boundaries controls the varistor electrical properties. Moreover, the amount of secondary phase formed by solid-state precipitation at the boundaries, if it occurs, is too low to affects the electrical property degradation, which is distinct from the ZnO varistor system. Considering the discussions above, a Schottky-type barrier, as in the models for ZnO-based varistors proposed by Gupta and Carlson,[12] can be ascribed as the most likely barrier at the SnO_2 grain boundary. Unlike the ZnO-based varistors, two SnO_2 grains grow and touch each other and the two barrier tops should touch each other, which has been confirmed by Bacelar *et al*[9] and Bueno *et al*.[23] The donor and donor-like ions ($Sn^{\cdot\cdot\cdot\cdot}_i, V^{\cdot\cdot}_O, Ta^{\cdot}_{Sn}$) extending from both sides of the grain boundary are compensated by the negatively charged ions ($Sn''_{Sn}, V''''_{Sn}, e', Co'_{Sn}, Ba''_{Sn}$) at the grain boundary interface. At the same time, the oxygen species adsorbed at the interface also are responsible for the Schottky barrier formation. The oxygen species can react with negative defects according to the following equations:

$$O_2 \longrightarrow O^{x}_{2(ad)}, \quad (6)$$

$$Ba''_{Sn} + 2O^{x}_{2(ad)} \longrightarrow Ba^{x}_{Sn} + 2O'_{2(ad)}, \quad (7)$$

$$Ba''_{Sn} + 2O'_{2(ad)} \longrightarrow Ba^{x}_{Sn} + 4O'_{(ad)}. \quad (8)$$

The adsorbed oxygen at the grain boundary captures electrons from negatively charged defects at the grain boundary and stays at the interface. This effect was confirmed by impedance analysis.[23] The electric transport occurs by tunnelling across the barriers and is responsible for the electrical nonlinearity of the varistors.

4. Conclusion

In conclusion, $BaCO_3$ additive has a great effect on electrical properties and dielectric properties of the SnO_2-based varistors. Barium can enhance the threshold voltage of SnO_2-based varistors. The sample with 1.00mol% $BaCO_3$ has the best nonlinear electrical property and the highest nonlinear coefficient (α=29.2) among the samples with different concentrations. A modified defect barrier model has been introduced to explain the formation of the grain-boundary barrier.

References

[1] Cerri J A, Leite E R, Gouvea D, Longo E and Varela J A 1996 *J. Am. Ceram. Soc.* **79** 799

[2] Castro M S and Aldao C M 1998 *J. Eur. Ceram. Soc.* **18** 2233

[3] Li C P, Wang J F, Su W B, Chen H C, Wang W X and Zhuang D X 2001 *Physica* B **307** 1

[4] Uematsu K, Terada A, Morimoto T, Uchida N and Saito K 1989 *J. Am. Ceram. Soc.* **72** 1070

[5] Fan J and Freer R 1997 *J. Mater. Sci.* **32** 415

[6] Yang S L and Wu J M 1995 *J. Mater. Res.* **10** 345

[7] Yang S L and Wu J M 1995 *J. Mater. Sci. Lett.* **10** 784

[8] Caballero A C, Valle F J, Villeqas M, Moure C, Duran P and Fernandez J F 2000 *J. Eur. Ceram. Soc.* **20** 2767

[9] Bacelar W K, Oliveira M M, Souza V C, Longo E, Leite E R and Varela J A 2002 *J. Mater. Sci.: Mater. Electron.* **13** 409

[10] Wang C M, Wang J F, Chen H C, Wang W X, Su W B, Zang G Z and Qi P 2003 *J. Phys.* D: *Appl. Phys.* **36** 3069

[11] Gupta T K 1990 *J. Am. Ceram. Soc.* **73** 1817

[12] Gupta T K and Carlson W G 1985 *J. Mater. Sci.* **20** 3487

[13] Mahan G D 1983 *J. Appl. Phys.* **54** 3825
[14] Eda K 1978 *J. Appl. Phys.* **49** 2964
[15] Antunes A C, Antunes S R M, Pianaro S A, Rocha M R, Longo E and Varela J A 1998 *J. Mater. Sci. Lett.* **17** 577
[16] Levinson L M and Philipp H R 1975 *J. Appl. Phys.* **46** 1332
[17] Hower P L and Gupta T K 1979 *J. Appl. Phys.* **50** 4847
[18] Clarke D R 1999 *J. Am. Ceram. Soc.* **82** 485
[19] Pianaro S A, Bueno P R, Longo E and Varela J A 1999 *Ceram. Int.* **25** 1
[20] Bueno P R, Leite E R, Oliveira M M, Orlandi M O and Longo E 2001 *Appl. Phys. Lett.* **79** 48
[21] Qi P, Wang J F, Chen H C, Su W B, Wang W X, Zang G Z and Wang C M 2003 *Acta Phys. Sin.* **52** 1752 (in Chinese)
[22] Wang C M, Wang J F, Chen H C, Su W B, Zang G Z and Qi P 2004 *Chin. Phys. Lett.* **21** 716
[23] Bueno P R, Pianaro S A, Pereira E C, Bulhoes L O S, Longo E and Varela J A 1998 *J. Appl. Phys.* **84** 3700